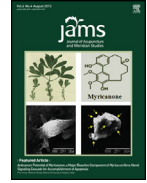


Available online at [www.sciencedirect.com](http://www.sciencedirect.com)

# Journal of Acupuncture and Meridian Studies

journal homepage: [www.jams-kpi.com](http://www.jams-kpi.com)

## RESEARCH ARTICLE

# Anticancer Potential of Myricanone, a Major Bioactive Component of *Myrica cerifera*: Novel Signaling Cascade for Accomplishing Apoptosis

Avijit Paul, Jayeeta Das, Sreemanti Das, Asmita Samadder,  
Anisur Rahman Khuda-Bukhsh\*

Cytogenetics and Molecular Biology Laboratory, Department of Zoology, University of Kalyani,  
Kalyani, India

Available online Jun 15, 2013

Received: Mar 1, 2013  
Revised: Apr 19, 2013  
Accepted: May 2, 2013

### KEYWORDS

apoptosis;  
cytochrome c;  
HepG2 cells;  
HSP70;  
myricanone;  
reactive oxygen species

### Abstract

Extract of *Myrica cerifera* bark has long been fruitfully used as a hepato-protective and anti-cancer drug in various complementary and alternative systems of medicine. Myricanone, its principal bioactive compound, had also been reported to have apoptosis-promoting ability. We evaluated its anti-cancer potential *in vitro* in HepG2 liver cancer cells and tried to understand the signal cascades involved in accomplishing apoptosis. Further, we ascertained by using a (3-(4, 5-dimethylthiazol-2-yl)-2, 5-diphenyltetrazolium bromide assay (MTT) assay if it had cytotoxic effects on normal noncancerous liver cells (WRL-68). We deployed various tools and protocols, like phase contrast, scanning electron and fluorescence microscopies, performed an annexinV-FITC/PI assay and cell cycle analysis, and estimated the reactive oxygen species (ROS) generation and mitochondrial membrane depolarization through flow cytometry. Further, analyses of cytochrome-c translocation and of HSP70 and caspase expressions were also done by using immunoblots and Enzyme linked immunosorbent assay (ELISA). Results revealed that myricanone induced apoptosis in HepG2 cells through generation of ROS, depolarization of the mitochondrial membrane, early release of cytochrome-c, down-regulation of HSP70 and activation of a caspase cascade; it had no, or insignificant, cytotoxic effects in WRL-68 cells *in vitro* and in mice *in vivo*. Thus, myricanone has great potential for use in formulating an effective drug against both hepatotoxicity and hepatocellular cancer.

\* Corresponding author. Cytogenetics and Molecular Biology Laboratory, Department of Zoology, University of Kalyani, Kalyani 741235, India.

E-mail: [prof\\_arkb@yahoo.co.in](mailto:prof_arkb@yahoo.co.in), [khudabukhsh\\_48@rediffmail.com](mailto:khudabukhsh_48@rediffmail.com) (A.R. Khuda-Bukhsh).

## 1. Introduction

The prevalence of cancer is increasing worldwide despite diagnostic and therapeutic advancements. Hepatocellular carcinoma (HCC) is the most common type of liver cancer. Treatment options for HCC are limited, because radiation therapies are not recommended owing to the severe damage they inflict on liver tissues, and chemotherapies are only regionally effective [1]. Moreover, nonselective distribution of drugs, enhanced drug toxicity, and undesirable side effects aggravate the challenges for chemotherapy.

Heat shock protein 70 (HSP70), a molecular chaperone, is abundantly expressed in malignant tumors of various origins, which promotes tumorigenesis via its prosurvival function. HSP70 is a major inhibitor of apoptosis induced by chemotherapeutic agents [2,3]. Therefore, the search is on for the development of a drug that should ideally have an antiproliferative effect, arrest cell cycle, and also induce apoptosis of cancer cells, either through the activation of caspase cascades or by blocking HSP70 and other anti-apoptotic genes.

Complementary and alternative medicine practices have become popular, particularly in oncology, to provide a better quality of life to cancer patients by alleviating their sufferings [4,5]. Medicinal plant extracts and their bioactive components that demonstrate significant potential as anticancer therapeutic agents owing to their ability to inhibit tumor growth, angiogenesis, and metastasis with minimal side effects [6] are being seriously explored. *Myrica cerifera* (Myricaceae), "wax myrtle" or "bayberry," is one of these important medicinal plants used in folk, ayurveda, and homeopathic systems of medicine for various ailments of the liver including jaundice and cancer [7]. This plant grows in the northern and central parts of America, Bermuda, and the Caribbean, and is used to treat dental problems, stomachache, and constipation, and is also used as a skin cleanser [8]. In addition, it has a marked action on the liver, particularly on jaundice. The plant contains several organic compounds including diarylheptanoids (myricanone), terpenoids, flavonoids, tannins, and phenols [9]. Many diarylheptanoids have anti-inflammatory effects in various cancer cells [10,11]. A preliminary screening for the antitumor effect of myricanone has been reported [12]; to our knowledge, however, the anticancer mechanism of myricanone has yet to be clearly established. No precise study has yet been conducted to delineate the molecular mechanism(s) of its possible anticancer effect on HCC cells, particularly in relation to mitochondrial membrane potential (MMP) and reactive oxygen species (ROS) accumulation; furthermore, how myricanone induces apoptosis through a well-organized signal cascade in cancer cells is not yet precisely known.

Therefore, the main objectives of the study were to test whether: (1) the isolated myricanone had any cytotoxicity against HepG2 cells without affecting the viability of normal liver cells (WRL-68) *in vitro*, (2) the isolated myricanone affected or modulated depolarization of MMP and generation of ROS leading to apoptosis in HepG2 cells, (3) apoptosis in HepG2 was mediated through cytochrome *c* release and HSP70 modulation, and finally, (4) myricanone had any cytotoxic or hepatoprotective effects in mice *in vivo*.

## 2. Materials and methods

### 2.1. Reagents

Dulbecco's modified Eagle's medium, fetal bovine serum, penicillin, streptomycin, neomycin (PSN) antibiotic, trypsin, and ethylenediaminetetraacetic acid were purchased from Gibco BRL (Grand Island, NY, USA). Propidium iodide, DAPI (4',6'-diamidino-2 phenyl indole), MTT [3-(4,5-dimethyl-thiazol-2-yl)-2, 5-diphenyltetrazolium bromide], and all other chemicals used were purchased from Sigma-Aldrich (St. Louis, MO, USA). All organic solvents used were of HPLC grade.

### 2.2. Isolation of bioactive fraction and identification of myricanone from crude ethanolic extract of *M. cerifera*

The ethanolic extract of *M. cerifera* is available in the market as a homeopathic mother tincture. It was purchased from HAPCO (B.B. Ganguly Street, Kolkata, India). Myricanone was isolated from the extract of *M. cerifera* by adopting the methods described by Matsuda et al [13,14] with slight modifications. Briefly, the extract was evaporated at 30 °C. The dried extract (22 g) was dissolved in methanol, and the methanol-soluble part was partitioned in an *n*-butanol/H<sub>2</sub>O (1:1 v/v) solvent system. The *n*-butanol soluble part was subjected to ordinary phase silica gel (230–400 μm mesh) column chromatography. The column was then eluted sequentially with chloroform/methanol (9:1 v/v) solvent system, and four fractions (F<sub>1</sub>, F<sub>2</sub>, F<sub>3</sub>, and F<sub>4</sub>) were collected (200 mL each). Of these fractions, F<sub>2</sub> showed maximum anticancer potential on initial trials (the others had relatively less potential). For this, the F<sub>2</sub> fraction was further subjected to ordinary phase silica gel column chromatography, then eluted with hexane/ethyl acetate (7:3 v/v) solvent system, and five subfractions (F<sub>2.1</sub>, F<sub>2.2</sub>, F<sub>2.3</sub>, F<sub>2.4</sub>, and F<sub>2.5</sub>) were collected (200 mL each). Then it was further purified using preparative thin layer chromatography and characterized through Fourier transform infrared (FTIR) and mass spectroscopy. The extraction procedure is summarized in Fig. 1.

### 2.3. Cell culture

Cancer cells of the human HCC cell line (HepG2), and normal liver cell line (WRL-68) were procured from the National Centre for Cell Science, Pune, India. Both types of cells were cultured in Dulbecco's modified Eagle's medium supplemented with 10% fetal bovine serum and 1% antibiotic (PSN) in a humidified incubator with 5% CO<sub>2</sub>.

### 2.4. Cell viability assay

The percentage of viable cells was assessed by following the standard protocol [15], prior to and after treatment with myricanone, at a concentration ranging from 20 μg/mL to 100 μg/mL at a 24-hour interval. Briefly, after 24 hours of myricanone treatment, cell viability was assessed using the MTT assay, and the IC<sub>50</sub> value was determined. The intracellular formazan crystals formed were solubilized in acidic isopropanol, and the absorbance of the solution was

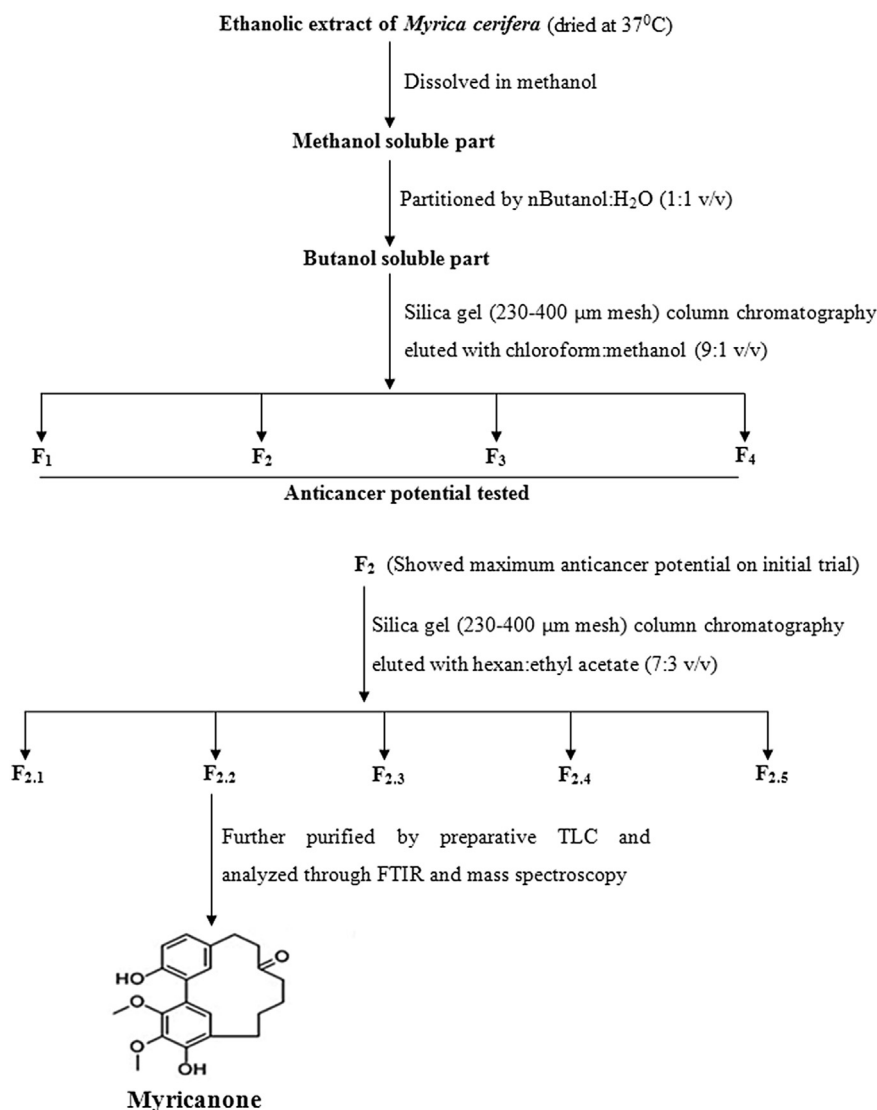


Figure 1 Schematic diagram of myricanone isolation procedure.

measured at 595 nm. Percentage viability was calculated as: optical density (OD) of drug treated sample/OD of control sample  $\times$  100.

## 2.5. Treatment types and dose selection

On the basis of MTT results and IC<sub>50</sub> value, three different doses (D1, 20 μg/mL; D2, 30 μg/mL; D3, 40 μg/mL) of myricanone were selected for further experiments. For HSP70 protein expression study, cells were preincubated with 10 μM Pifithrin-μ (HSP70 inhibitor) [16] for 2 hours prior to drug treatment. Control groups received only media without any treatment.

## 2.6. Assessment of apoptosis

### 2.6.1. Scanning electron microscopic and phase contrast microscopic analyses

Control and treated cells were washed with phosphate-buffered saline (PBS) and fixed with 2.5% glutaraldehyde for 2 hours. The cells were then washed three times with PBS and placed in desiccators overnight. Next, the cells were observed

separately under phase contrast (Leica Microsystems CMS GmbH, Ernst-Leitz-Straße 17-37, Wetzlar, D-35578 Germany) and scanning electron microscopes (S530-Hitachi, Tokyo, Japan).

### 2.6.2. Nucleosomal fragmentation analysis

Control and treated cells were washed with PBS and stained with 10 μg/mL DAPI for 10 minutes at 37 °C. The images of stained cells were taken under a fluorescence microscope (Leica, Germany).

### 2.6.3. Annexin V-FITC/PI assay

In order to evaluate apoptosis and necrosis, externalization of phosphatidylserine during apoptosis and leakage from necrotic cells was observed by Annexin V-FITC/PI (propidium iodide) dual staining using the standard protocol [15]. Differentiation of cell population was done on flow cytometer (BD FACS Calibur, San Jose, CA, USA) and was assessed as follows: (a) viable cancer cells (Annexin -ve; PI -ve), (b) early apoptotic cancer cells (Annexin +ve; PI -ve), (c) late apoptotic cancer cells (Annexin +ve; PI +ve), (d) necrotic cells (PI +ve). Samples were analyzed using the Cyflogic (version 1.2.1, Cyflogic Team,

Turku, Finland) software, and determination was based on the mean fluorescence intensity of 10,000 events.

## 2.7. Cell cycle analysis

After 24 hours of myricanone treatment, cells were suspended in PBS and fixed by the addition of 70% ice cold methanol. The fixed cells were harvested and washed with PBS; next, RNase (1  $\mu\text{g}/\mu\text{L}$ ) was added to the samples, which were then resuspended in PI stain (10  $\mu\text{g}/\text{mL}$ ). The fluorescence was measured at 585 nm. Flow cytometric data were analyzed using Cyflogic (version 1.2.1) software.

## 2.8. Detection of intracellular ROS accumulation and change in MMP ( $\Delta\Psi\text{m}$ )

Intracellular ROS accumulation and change in  $\Delta\Psi\text{m}$  were evaluated through fluorescence microscopy and flow cytometry as described elsewhere [15]. Briefly, intracellular ROS accumulation and change in  $\Delta\Psi\text{m}$  were evaluated by fluorescence microscopy. Control and treated cells were fixed in 70% ethanol and incubated for 30 minutes in dark with 20  $\mu\text{M}$   $\text{H}_2\text{DCFDA}$  (2',7'-dichlorodihydrofluorescein dichlorodihydrofluorescein diacetate) and 10  $\mu\text{M}$  Rhodamine 123, respectively. Then, cells were analyzed under fluorescence microscope.

For the quantitative estimation of ROS and  $\Delta\Psi\text{m}$ , cells were fixed in 70% ethanol and incubated with 20  $\mu\text{M}$   $\text{H}_2\text{DCFDA}$ . And 10  $\mu\text{M}$  Rhodamine 123, respectively, for 30 minutes in the dark. The fluorescence intensity of dye was determined by flow cytometry using FL1-H filter. Data were analyzed using Cyflogic (version 1.2.1) software.

## 2.9. Preparation of cell lysate

Briefly,  $1 \times 10^6$  cells/mL were lysed in 20  $\mu\text{L}$  ice-cold lysis buffer [10 mM Tris-hydrochloride (HCl), 1 mM magnesium chloride, 1 mM ethylenediaminetetraacetic acid, 0.1 mM phenylmethylsulfonyl fluoride, 5 mM  $\beta$ -mercaptoethanol, 0.5% CHAPS (3-[(3-cholamidopropyl)dimethylammonio]-1-propanesulfonate), 10% glycerol]. Cells were incubated for 30 minutes on ice and centrifuged for 20 minutes at  $8000 \times g$  at 4 °C, and the supernatants were collected and stored at -20 °C for further use.

## 2.10. Cytochrome c activity assay

The cellular lysate was used for the quantification of cytochrome c activity by indirect enzyme-linked immunosorbent assay (ELISA) as described earlier [17]. Briefly, cells were coated with anticytochrome c primary antibody and blocked by 3% bovine serum albumin (BSA) solution. After the secondary antibody incubation, *para*-nitrophenylphosphate was used as a color developer, and color intensity was measured at 405 nm with respect to blank.

## 2.11. Immunofluorescence study for detection of HSP70 expression

Immunofluorescence study was performed using anti-HSP70 primary antibody by following the standard protocol [15].

Briefly, at the end of treatments, cells were fixed in 3% paraformaldehyde for 1 hour. Cells were then permeabilized with 0.2% CHAPS {3-[(3-cholamidopropyl)dimethylammonio]-1-propane sulfonate} in PBS for 2 minutes, and cells were blocked in 3% BSA with 0.2% Tween-20 for 30 minutes. Cells were then incubated overnight at 4 °C with anticytochrome c primary antibody and observed under fluorescence microscope after incubating with IgG-FITC secondary antibody.

## 2.12. Preparation of cytosolic and mitochondrial fractions

Control and treated HepG2 cells were collected, washed with ice-cold PBS, resuspended in buffer A (10 mM Tris-MOPS pH 7.4, 200 mM sucrose, 1 mM EGTA (ethylene glycol tetraacetic acid), 1 mg/mL BSA, 1 mM DTT (Dithiothreitol)) and lysed by homogenization. The suspension was centrifuged at  $1000 \times g$  for 10 minutes at 4 °C. The resulting supernatant was centrifuged at  $10,000 \times g$  for 15 minutes to pellet mitochondria. Cytosolic fraction (supernatant) was obtained by centrifugation at  $12,000 \times g$  for 1 hour at 4 °C [18].

## 2.13. Immunoblot analysis

To analyze the expressions of different proteins, immunoblot analysis was done using anti-HSP70, cytochrome c, Apaf-1, caspase-9, and caspase-3 antibodies by following the standard protocol [18]. Alkaline phosphatase (ALP)-conjugated secondary antibodies were used for this purpose. Bound antibodies were developed by 5-bromo-4-chloro-3-indolyl phosphate/nitro blue tetrazolium (BCIP-NBT), and the band intensity was measured using Image J software (National Institute of Health, MD, USA). GAPDH was used as the housekeeping protein.

## 2.14. Reverse transcriptase-polymerase chain reaction analysis

Semiquantitative reverse transcriptase-polymerase chain reaction (RT-PCR) was performed as previously described [17]. The sequences of the forward and reverse primers used for specific amplifications were as follows: Bcl-2: (Fwd 5'-GTGACTTCCGATCAGGAAGG-3' and Rev 5'-CTTCCAGACATTCGGAGACC-3'); Bax: (Fwd 5'-AGTAACATGGAGCTGCAGAGG-3' and Rev 5'-ATGGTCTGATCAGTCCGG-3') and GAPDH (Fwd 5'-CCCACTAACATCAAATGGGG-3' and Rev 5'-CCTCCACAATGCAAAGTT-3'). The fluorescence intensity of the bands was measured using the Image J software.

## 2.15. Animals

Randomized mice (*Mus musculus*) of Swiss albino strain, weighing between ~20 g and 25 g, were selected and housed under standard environmental conditions at ambient temperature of ~25 °C. The guidelines approved by the Animal Ethics Committee, University of Kalyani, were followed in this experiment. Animals were cared for and supplied with food and water *ad libitum*. After 1 week of acclimatization, the mice were used for the experiments. The body weight and food intake data of mice were

recorded prior to the start and at the end (after 14 days) of the experiment.

### 2.15.1. Acute toxicity studies in mice

A group consisting of five mice each is considered optimum for conducting *in vivo* experimental research work [19]. For acute toxicity test, mice divided into three separate groups ( $n = 5$ ) were fed, respectively, with 50 mg/kg, 75 mg/kg, and 100 mg/kg body weight (bw) of myricanone dissolved in water. The mortality rate, clinical sign of acute toxicity, and behavioral changes in mice were monitored over the 14-day period.

### 2.15.2. Biochemical analysis of serum enzymes

The mice from each group were sacrificed, and blood was collected by cardiac puncture. The activities of alanine aminotransferase (ALT) and aspartate aminotransferase (AST) were analyzed with a spectrophotometer according to the standard protocols [20]. The activity of ALP was determined using the appropriate diagnostic kit (Crest Biosystems, Verna, Goa, India).

## 2.16. Statistical analysis

The results of all experiments are presented as mean [ $\pm$ standard error (SE)] of values of three independent experiments. Statistical analysis was performed using Student *t* test or one-way analysis of variance (ANOVA; Fisher's least significant difference (LSD) *post-hoc* test), where  $p < 0.05$

(\*),  $p < 0.01$  (\*\*), and  $p < 0.001$  (\*\*\*) versus control were considered significant.

## 3. Results

### 3.1. Characterization of chromatographic fraction

Fourier transform infrared (FTIR) and mass spectroscopic data showed the F<sub>2.2</sub> fraction to be rich in myricanone [C<sub>21</sub>H<sub>24</sub>O<sub>5</sub>, MS  $m/z$ : 356(M-Na)<sup>-</sup>] [14], which was then selected for further study. The FTIR data (peak at 3317/cm represents the OH group, 2854/cm represents the CH<sub>2</sub> group, 1713/cm represents the C=O group, 1505/cm–1110/cm represents the aromatic CH group, aliphatic CH<sub>3</sub> group) of the purified myricanone are shown in Fig. 2A.

### 3.2. Effects of myricanone on cell viability

Results of the MTT assay revealed that myricanone had significant cytotoxic effects on HepG2 cells, whereas it had no such significant cytotoxic effect on the normal liver cells (WRL-68) *in vitro*. The cell viability was gradually decreased from the minimal drug concentration to the higher ones. The highest dose of myricanone (100  $\mu$ g/mL) showed 12.41% cell viability in HepG2, whereas it was 89.27% for WRL-68 cells. The IC<sub>50</sub> value of myricanone in HepG2 cells was 32.46  $\mu$ g/mL (Fig. 2B).

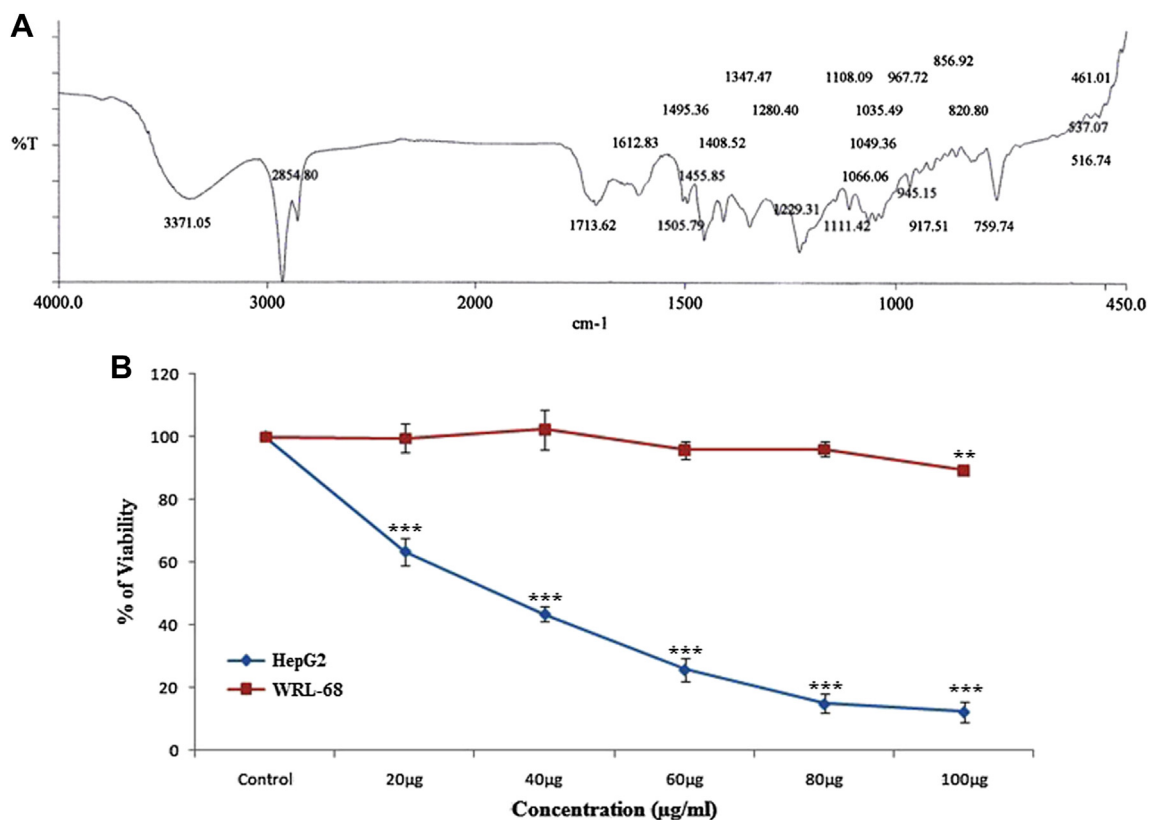


**Figure 2** (A) Fourier transform infrared (FTIR) spectrum of isolated myricanone. (B) Cytotoxic effects of myricanone on HepG2 and WRL-68 cells after 24 hours of treatment. Cell viability was measured by MTT (3-(4,5-dimethyl-thiazol-2-yl)-2, 5-diphenyltetrazolium bromide) assay (\*\* $p < 0.01$  and \*\*\* $p < 0.001$  vs control was considered significant).

### 3.3. Effect on morphological changes and nucleosomal fragmentation in HepG2 cells

The morphological changes in myricanone-treated HepG2 cells were analyzed through phase contrast and scanning electron microscopes (Fig. 3A and B). Typical apoptotic characteristics such as cellular distortion, cell shrinkage, and membrane blebbing were observed in a dose-dependent manner. Cellular distortion was found to be most frequent at the highest dose.

The untreated HepG2 cells did not take positive staining with DAPI and showed no cells with visible chromatin condensation. However, with different concentrations of treatment, cells with chromatin condensation appeared to increase in number along with the increase in dose (Fig. 3C).

### 3.4. Effect on apoptotic percentage of cells

Apoptosis was confirmed with Annexin V-FITC/PI dual staining using FACSCalibur (BD Bioscience). After treatment with myricanone, both early and late apoptotic cells significantly increased in a dose-dependent manner. The number of apoptotic cells was increased in a dose-dependent manner compared to their controls, whereas increase in necrotic percentage was negligible in all drug-treated cells (Fig. 3D).

### 3.5. Effect on cell cycle progression

Cell cycle analysis on D1, D2, and D3 of myricanone-treated HepG2 cells revealed that (Fig. 4) the cells passed through the mitotic division but were arrested at the G<sub>0</sub>/G<sub>1</sub> phase, thereby indicating that the diarylheptanoid compound acted as a G<sub>0</sub>/G<sub>1</sub> phase inhibitor, as also reported in another study on curcumin [21]. D3 caused higher G<sub>0</sub>/G<sub>1</sub> phase arrest (53.32%) compared to control (42.69%) in HepG2 cells with consistent decrease in G<sub>2</sub>/M phase (control, 35.64%; D3, 22.42%).

### 3.6. Effect on ROS generation and depolarization of MMP ( $\Delta\Psi_m$ ) in HepG2 cells

A time-dependent ROS generation was observed by DCFDA staining. The control cells showed low green fluorescence, whereas the cells treated with drug showed gradual increase in fluorescence intensity along with increasing time, reflecting the accumulation of ROS. Quantitative data obtained by flow cytometer would also convincingly support the previous observation, as the generation of ROS was found to be increased along with the increase in the period of drug exposure (Fig. 5A).

Depolarization of MMP was measured both qualitatively and quantitatively by Rhodamine 123 staining. The fluorescence

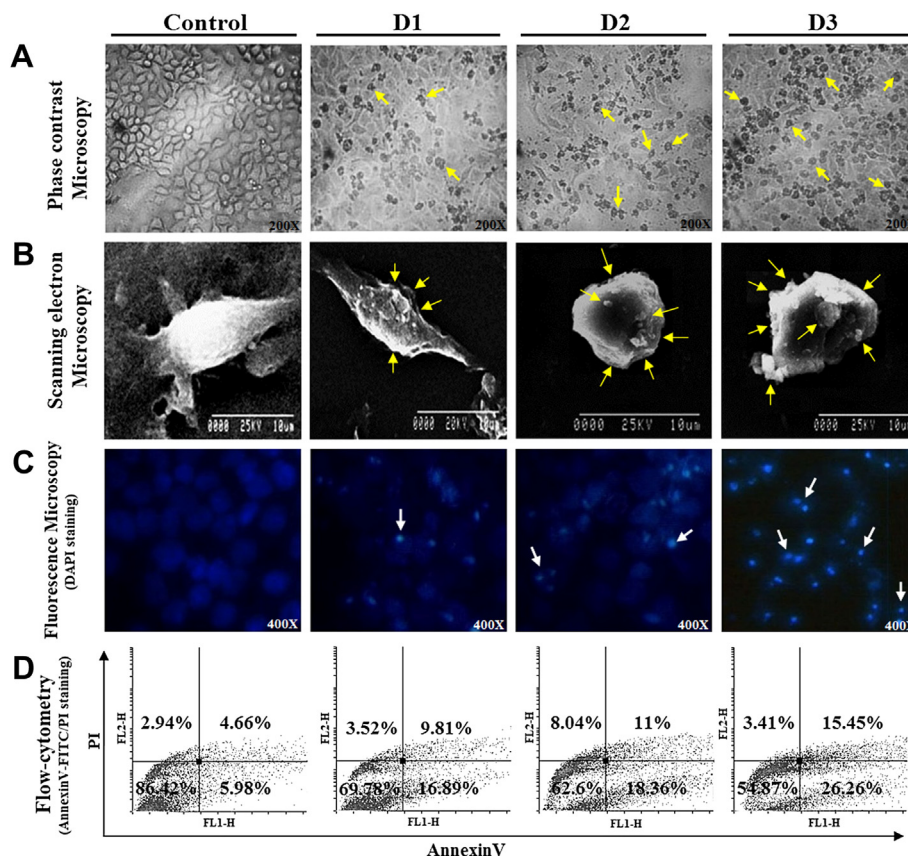


**Figure 3** Myricanone induced apoptosis in HepG2 cells at different doses (D1, D2, and D3). (A) Overall morphological features of HeLa cells observed under phase contrast microscopy; arrows indicate apoptotic cells. (B) Morphology of HeLa cells observed under scanning electron microscopy. (C) Chromatin condensation observed under fluorescence microscopy by DAPI staining; arrows show nuclear fragmentation. (D) Flow cytometric analysis of apoptosis by Annexin V-FITC/PI staining.

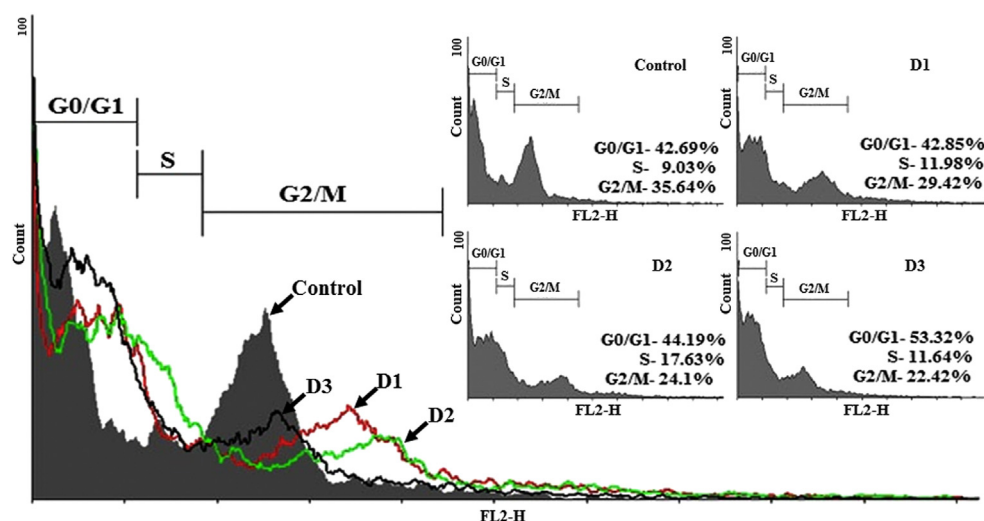


**Figure 4** Flow-cytometric analysis of cell cycle at different doses of myricanone. Overlay diagram shows changes in cell cycle phase with respect to control.

intensity of treated cells was reduced with respect to control cells in a time-dependent manner, thereby reflecting the loss of  $\Delta\Psi_m$ , which was also confirmed by flow cytometric analysis, showing a marked decrease in fluorescence intensity after myricanone (D2) treatment (Fig. 5B).

### 3.7. Effect on translocation of cytochrome c from mitochondria to cytosol in HepG2 cells

Translocation of cytochrome c is an important event at the early stage of the apoptosis pathway. To determine whether myricanone played a role in the release of cytochrome c from mitochondria into cytosol, the location of cytochrome c was analyzed. Indirect ELISA showed that myricanone (D2) caused the release of cytochrome c from mitochondria into cytosol in a time-dependent manner. The result revealed that the release of cytochrome c into cytosol started mainly after 4 hours of myricanone exposure and the release consistently increased up to 12 hours, and thereafter a constant release (Fig. 5C) was maintained. A dose-dependent increase was also confirmed by immunoblot analysis (Fig. 5D), as the expression of cytochrome c was decreased in mitochondrial fraction along with a corresponding increase in cytosolic fraction with respect to control cells (Fig. 5D).

### 3.8. Effect on regulation of HSP70 expression in HepG2 cells

In order to determine whether HSP70 played any role in myricanone-induced apoptosis in HepG2 cells, HSP70 activity was assessed by immunofluorescence and immunoblot analysis. Immunofluorescence analysis showed that the fluorescence intensity of HSP70 was decreased in a time-dependent fashion with respect to control (Fig. 6A). Densitometric analysis of immunoblot showed similar down-regulation of HSP70 by 0.52-fold (52%) after 24 hours in a time-dependent manner with respect to control cells (Fig. 6B). To confirm the effect of HSP70 expression on

myricanone-treated cell viability, HepG2 cells were pre-treated with pifithrin- $\mu$  (HSP70 inhibitor). Immunoblot analysis revealed that there was a 0.51-fold (51%) decrease in D2-treated cells, whereas a 0.47-fold (47%) decrease in the case of pifithrin- $\mu$  only treatment and a 0.42-fold (42%) decrease in combined pifithrin- $\mu$  and drug treatment after 24 hours with respect to control (Fig. 6C) were noted. Immunoblot analysis of HSP70 expression was also down-regulated after 24 hours of treatment (Fig. 6D) in a dose-dependent manner with respect to untreated cells.

### 3.9. Effect on expression of apoptotic signal proteins

Expression of Apaf-1, caspase-9, and caspase-3 was increased by drug administration in a dose-dependent manner. For Apaf-1, the expression was enhanced by 1.12-, 1.45-, and 1.61-fold for D1, D2, and D3 drug doses, respectively. In the case of caspase-9, the expression was enhanced by 1.28-, 1.58-, and 1.79-fold, respectively, and for caspase-3, the expression was increased by 1.09-, 1.23-, and 1.31-fold, respectively, with the respective drug dose (Fig. 6E).

### 3.10. Effect on mRNA expression of pro- and antiapoptotic genes

The results of RT-PCR showed that myricanone treatment had up-regulated the mRNA expression of proapoptotic gene Bax, whereas antiapoptotic Bcl-2 gene expression was down-regulated in a dose-dependent manner after 24 hours of treatment (Fig. 6F).

### 3.11. Effect on general toxicity and enzyme biomarkers in mice *in vivo*

No significant changes in food intake, mortality, occurrence of abnormal clinical signs, symptoms, gain or loss of body weight, organ weight, etc., were observed in respect of acute toxicity analysis of myricanone (at tested doses) in

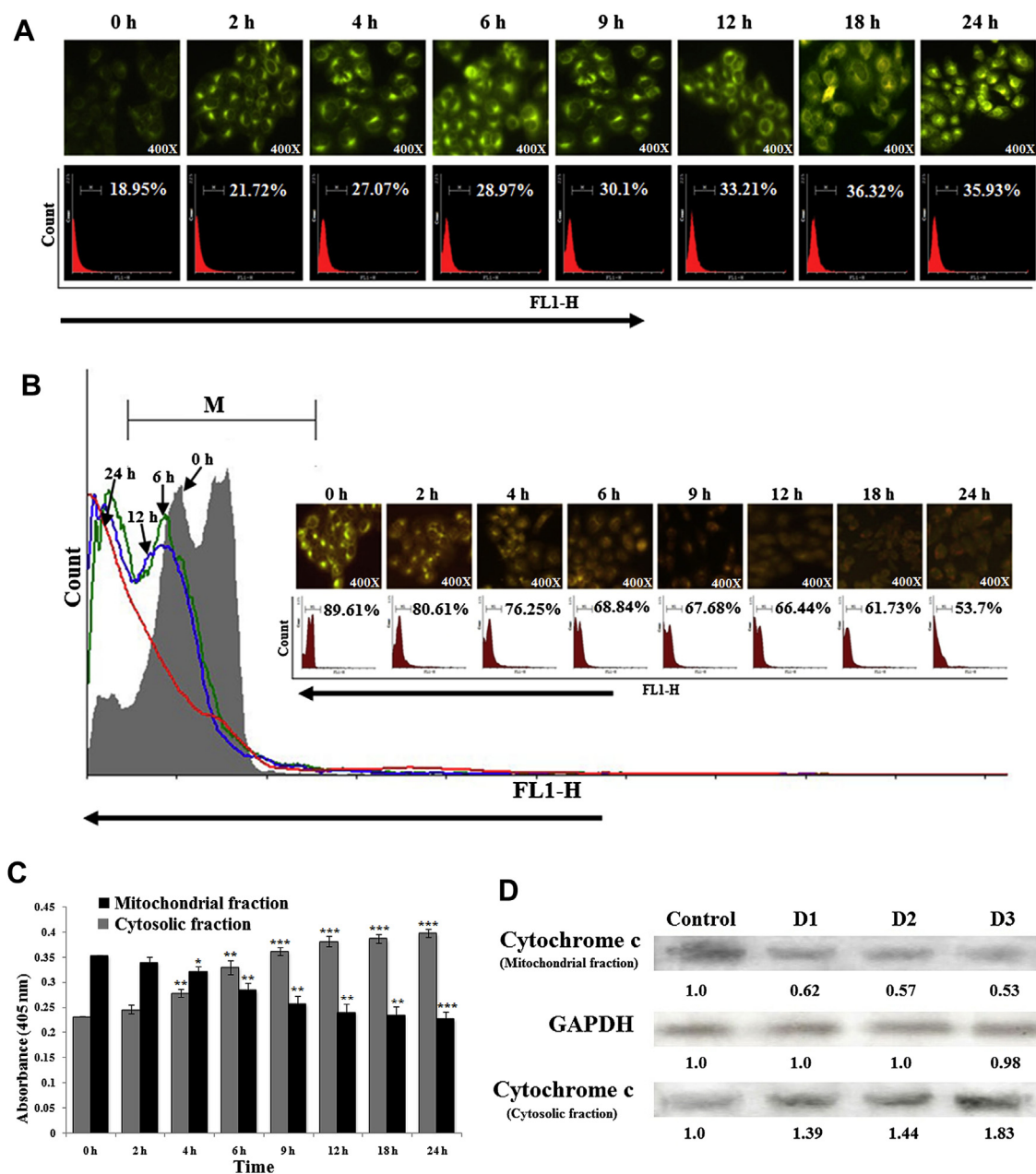


**Figure 5** Measurement of reactive oxygen species (ROS), mitochondrial membrane potential (MMP), and cytochrome *c* translocation. (A) Fluorescence photomicrograph by DCFDA staining. (B) Fluorescence intensity by FACSCalibur using Rhodamine123 dye for the detection of MMP. (C) Cytochrome *c* assay by enzyme-linked immunosorbent assay to detect translocation of cytochrome *c* from mitochondria into cytosol after myricanone exposure (\* $p < 0.05$ , \*\* $p < 0.01$  and \*\*\* $p < 0.001$  vs control was considered significant.). (D) Immunoblot analysis to show translocation of cytochrome *c* from mitochondria to cytosol. *GAPDH* was used as a housekeeping gene.

mice over the entire experimental period (14 days). No such significant changes in the serum activity levels of ALT, AS, and ALP were also observed in myricanone-treated mice after the experimental period (Table 1).

#### 4. Discussion

After observing the considerable hepatoprotective effects of crude ethanolic extracts from the bark of *M. cerifera* in our laboratory (data not shown), we became more interested in examining if its major bioactive compound,

myricanone, could also demonstrate such properties, and if it did, to learn in more detail about its signaling cascade to accomplish apoptosis. The present findings showed that myricanone inhibited the growth of HepG2 cells in a dose-dependent manner, whereas it had little or no cytotoxicity on normal liver cells (WRL-68). The ability to induce apoptosis in cancer cells is considered one of the hallmark features of many anticancer drugs. In the current study, myricanone induced an apoptotic response in HepG2 cells as manifested in the morphological changes, with progressive detachment of cells, cytoplasmic shrinkage, membrane blebbing, and formation of apoptotic bodies containing

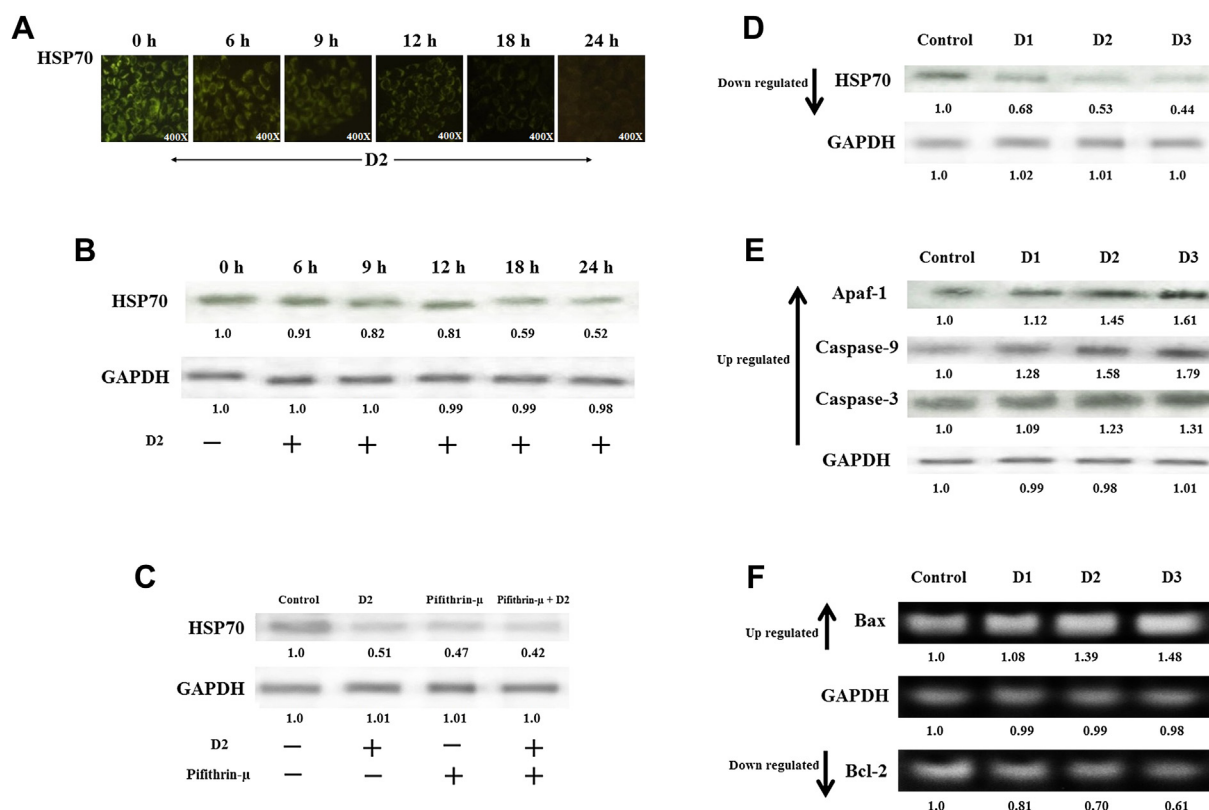


**Figure 6** (A) Immunofluorescence study of HSP70 protein reveals that the fluorescence intensity was gradually decreased with an increase in time. (B) Time-dependent down-regulation of HSP70 expression was also observed by immunoblot study. (C) HSP70 activity was also detected by immunoblot study using Pifithrin- $\mu$  (HSP70 inhibitor), showing consequent down-regulation of HSP70 expression after drug treatment. (D) Immunoblot expression of HSP70 showed significant down-regulation after myricanone treatment in a dose-dependent manner. (E) Immunoblot expression of Apaf-1, caspase-9, and caspase-3 showed significant up-regulation of Apaf-1, caspase-9, and caspase-3 after myricanone treatment in a dose-dependent manner. (F) Reverse transcriptase-polymerase chain reaction (RT-PCR) analysis of mRNA expression of Bax and Bcl-2 showed up-regulation of Bax and down-regulation of Bcl-2 activity after myricanone treatment. *GAPDH* acts as a house keeping gene. The intensity of control was normalized to 1, and the intensity of each band from treated cells is compared to the control.

condensed and fragmented chromatin. The analysis of the apoptotic phenomenon was further confirmed by Annexin V-FITC/PI assay, where an increase in the population of cells undergoing apoptosis was noted in a dose-dependent manner. Concomitantly, the growth rate of the cells was also found to be reduced at the G0/G1 phase after myricanone treatment, which is in agreement with earlier findings where curcumin, a diarylheptanoid, showed cell cycle arrest at the G0/G1 phase in breast cancer cells [21].

By contrast, increase in the generation of ROS has long been implicated in the apoptotic response induced by several anticancer agents [22,23]. MMP also plays a critical role in apoptosis by releasing apoptotic factors. Recently,

chemotherapeutic drugs targeting mitochondria has been hailed as a landmark discovery in cancer therapy [24]. The present study reveals that treatment with myricanone increases cellular ROS accumulation with concomitant decrease in MMP. This shows that myricanone-induced apoptosis was possibly mediated through ROS generation and activation of the mitochondria-dependent cell death pathway. Accumulation of ROS and depolarization of MMP are concurrent processes that normally induce mitochondria to release cytochrome *c* to the cytoplasm. It is reported that cytochrome *c* released from mitochondria triggers caspase activation, which could be mediated through the direct or indirect action of ROS [25]. In the

**Table 1** Effect of myricanone on the activity of different serum enzymes of mice after 14 days.

Group	ALT (units/mL)	AST (units/mL)	ALP (KA units/mL)
Control	13.29 $\pm$ 0.84	12.12 $\pm$ 0.73	5.76 $\pm$ 0.35
Myricanone (50 mg/kg bw)	14.98 $\pm$ 1.44	14.46 $\pm$ 0.1.25	6.28 $\pm$ 0.22
Myricanone (75 mg/kg bw)	13.84 $\pm$ 0.89	13.59 $\pm$ 0.95	5.78 $\pm$ 0.35
Myricanone (100 mg/kg bw)	13.56 $\pm$ 1.14	14.34 $\pm$ 0.72	6.0 $\pm$ 0.33

Data are presented as mean  $\pm$  standard error of five mice ( $n = 5$ ) per group.

ALP = alkaline phosphatase; ALT = alanine aminotransferase; AST = aspartate aminotransferase.

present study, the early release of cytochrome *c* after myricanone treatment would further lend support to this contention. The release of cytochrome *c* into cytosol peaked after 12 hours of treatment, which coincided with a marked increase in ROS formation and a decrease in MMP. This would indicate that the initiation of cytochrome *c* disposal might be dependent on ROS generation with MMP disruption and could thereby initiate apoptosis after myricanone treatment.

HSP70 is an important suppressor of apoptosis. Under normal conditions, HSP70 proteins function as molecular chaperones. When the cancer cells become resistant to chemotherapeutic drugs, the synthesis of stress-inducible HSP70 in the cancer cells enhances their ability to survive [26]. The cytoprotective role of HSP70 is attributed to its chaperone activity. It has been demonstrated that direct binding of Apaf-1 to HSP70 prevents the recruitment of procaspase-9 to form the apoptosome complex [27]. The results of our time-dependent immunofluorescence and immunoblot studies suggest that myricanone inhibited HSP70 expression and thus enhanced the release of cytochrome *c* into cytosol and consequently up-regulated the Apaf-1 expression to form the apoptosome complex and initiated apoptosis through the caspase-dependent pathway. Moreover, the expressions of caspase-9 and caspase-3 were also increased in a dose-dependent manner. Thus, the present study demonstrates that myricanone treatment altered the levels of HSP70 that could lead to the loss of control of cell growth and exerted inhibitory effects on apoptosis in HepG2 cells.

The Bcl-2 family proteins are known to be a regulator of mitochondrial membrane permeability and polarization, and also the regulator of the release of cytochrome *c* in cytosol from mitochondria to initiate apoptosis [28]. Significant modulations in Bax and Bcl-2 expressions upon myricanone exposure indicate an ultimate imbalance of the Bax/Bcl-2 ratio that leads to HepG2 cells toward apoptosis, through MMP depolarization.

As toxicity is generated by most of the chemotherapeutic drugs used, any anticancer drug having no or insignificant effects either on normal cells *in vitro* or on test animals *in vivo*, is considered acceptable and safe for use for a considerable period. Our *in vivo* study showed that myricanone did not show any palpable cytotoxic effect (at the tested dose) on mice. The enzyme biomarkers (ALT, AST, and ALP) also supported the antihepatotoxic role of myricanone *in vivo*.

In summary, myricanone triggered apoptotic cell death in HepG2 cells through generation of ROS and early release of cytochrome *c* to cytosol from mitochondria by depolarization of MMP, suppression of HSP70 activity, and elevating mitochondria-dependent caspase activity to induce apoptosis in cancer cells. Thus, myricanone has the requisite qualities and potential to be considered as a suitable candidate in formulating an effective anticancer therapy, particularly that affecting the liver.

## Conflict of interest

The authors declare that there are no conflict of interest.

## Acknowledgments

The authors gratefully acknowledge Boiron Laboratory, Lyon, France, for providing partial financial support to Professor A.R. Khuda-Bukhsh for this work.

## References

1. Newell P, Villanueva A, Friedman SL, Koike K, Llovet JM. Experimental models of hepatocellular carcinoma. *J Hepatol.* 2008;48:858–79.
2. Jaattela M. Heat shock proteins as cellular lifeguards. *Ann Med.* 1999;31:261–71.
3. Ciocca DR, Calderwood SK. Heat shock proteins in cancer: diagnostic, prognostic, predictive and treatment implications. *Cell Stress Chaperones.* 2005;10:86–103.
4. Ban JO, Hwang IG, Kim TM, Hwang BY, Lee US, Jeong HS, et al. Anti-proliferate and pro-apoptotic effects of 2,3-dihydro-3,5-dihydroxy-6-methyl-4H-pyranone through inactivation of NF-KB in human colon cancer cells. *Arch Pharm Res.* 2007;30:1455–63.
5. Banerjee S, Manna S, Mukherjee S, Pal D, Panda CK, Das S. Black tea polyphenols restrict benzopyrene-induced mouse lung cancer progression through inhibition of Cox-2 and induction of caspase-3 expression. *Asian Pac J Cancer Prev.* 2006;7:661–6.
6. Cragg GM, Newman DJ, Snader KM. Natural products in drug discovery and development. *J Nat Prod.* 1997;60:52–60.
7. Boericke W. *Pocket Manual of Homeopathic Material Medica and Repertory.* New Delhi: B. Jain Publishers; 2002:514.
8. Lentz DL, Clark AM, Hufford CD, Meurer-Grimes B, Passreiter CM, Cordero J, et al. Antimicrobial properties of Honduran medicinal plants. *J Ethnopharmacol.* 1998;63:253–63.
9. Paul BD, Rao GS, Kapadia GJ. Isolation of myricadiol, myricitrin, taraxerol, and taraxerone from *Myrica cerifera* L. root bark. *J Pharm Sci.* 1974;63:958–9.
10. Akihisa T, Taquchi Y, Yasukawa K, Tokuda H, Akazawa H, Suzuki T, et al. Acerogenin M, a cyclic diarylheptanoid, and other phenolic compounds from *Acer nikoense* and their anti-inflammatory and anti-tumor-promoting effects. *Chem Pharm Bull (Tokyo).* 2006;54:735–9.
11. Lee CS, Jang ER, Kim YJ, Myung SC, Kim W, Lee MW. Diarylheptanoid hirsutenone enhances apoptotic effect of TRAIL on epithelial ovarian carcinoma cell lines via activation of death receptor and mitochondrial pathway. *Investigational New Drugs.* 2012;30:548–57.
12. Ishida J, Kozuka M, Wang H, Konoshima T, Tokuda H, Okuda M, et al. Antitumor-promoting effects of cyclic diarylheptanoids on Epstein–Bar virus activation and two-stage mouse skin carcinogenesis. *Cancer Lett.* 2000;159:135–40.
13. Matsuda H, Yamazaki M, Matsuo K, Asanuma Y, Kubo M. Anti-androgenic activity of myricae cortex—isolation of active constituents from bark of *Myrica rubra*. *Biol Pharm Bull.* 2001;24:259–63.
14. Matsuda H, Morikawa T, Tao J, Ueda K, Yoshikawa M. Bioactive constituents of Chinese natural medicines: VII. Inhibitors of degranulation in RBL-2H3 cells and absolute stereo structures of three new diarylheptanoid glycosides from the bark of *Myrica rubra*. *Chem Pharm Bull.* 2002;50:208–15.
15. Biswas R, Mandal SK, Dutta S, Bhattacharyya SS, Boujedaini N, Khuda-Bukhsh AR. Thujone-rich fraction of *Thuja occidentalis* demonstrates major anti-cancer potentials: evidences from *in vitro* studies on A375 cells. *Evid Based Complement Altern Med.* 2011;2011:568148.

16. Leu JI, Pimkina J, Frank A, Murphy ME, George DL. A small molecule inhibitor of inducible heat shock protein 70. *Mol Cell*. 2009;36:15–27.
17. Chakraborty D, Samadder A, Dutta S, Khuda-Bukhsh AR. Anti-hyperglycemic potentials of a threatened plant, *Helonias dioica*: antioxidative stress responses and the signaling cascade. *Exp Biol Med*. 2012;237:64–76.
18. Das S, Das J, Samadder A, Boujedaini N, Khuda-Bukhsh AR. Apigenin-induced apoptosis in A375 and A549 cells through selective action and dysfunction of mitochondria. *Exp Biol Med*. 2012;237:1433–48.
19. Ghosh D, Choudhury ST, Ghosh S, Mandal AK, Sarkar S, Ghosh A, et al. Nanocapsulated curcumin: oral chemopreventive formulation against diethylnitrosamine induced hepatocellular carcinoma in rat. *Chem Biol Interact*. 2012;195:206–14.
20. Reitman S, Franckals S. A colorimetric method for the determination of serum glutathione oxaloacetate transaminase and glutamic-pyruvic transaminases. *Am J Clin Pathol*. 1957;28:56–63.
21. Li H, Jin L, Wu F, Li X, You J, Cao Z, et al. Effect of curcumin on proliferation, cell cycle, and caspases and MCF-7 cells. *Afr J Pharm Pharmacol*. 2012;6:864–70.
22. Antosiewicz J, Herman-Antosiewicz A, Marynowski SW, Singh SV. c-Jun NH(2)-terminal kinase signaling axis regulates diallyl trisulfide-induced generation of reactive oxygen species and cell cycle arrest in human prostate cancer cells. *Cancer Res*. 2006;66:5379–86.
23. Su YT, Chang HL, Shyue SK, Hsu SL. Emodin induces apoptosis in human lung adenocarcinoma cells through a reactive oxygen species-dependent mitochondrial signaling pathway. *Biochem Pharmacol*. 2005;70:229–41.
24. Fulda S, Galluzzi L, Kroemer G. Targeting mitochondria for cancer therapy. *Nat Rev Drug Discov*. 2010;9:447–64.
25. Simon HU, Yehia AH, Levi-Schaffer F. Role of reactive oxygen species (ROS) in apoptosis induction. *Apoptosis*. 2000;5:415–8.
26. Samali A, Cotter TG. Heat shock proteins increase resistance to apoptosis. *Ex Cell Res*. 1996;223:163–70.
27. Beere HM, Wolf BB, Cain K, Mosser DD, Mahboubi A, Kuwana T, et al. Heat-shock protein 70 inhibits apoptosis by preventing recruitment of procaspase-9 to the Apaf-1 apoptosome. *Nat Cell Biol*. 2000;2:469–75.
28. García-Sáez AJ. The secrets of the Bcl-2 family. *Cell Death Differ*. 2012;19:1733–40.